



Mequindox-Induced Kidney Toxicity Is Associated With Oxidative Stress and Apoptosis in the Mouse

Qianying Liu¹, Zhixin Lei¹, Jingchao Guo², Aimei Liu², Qirong Lu², Zainab Fatima², Haseeb Khaliq², Muhammad A. B. Shabbir², Muhammad Kashif Maan², Qinghua Wu^{3,4}, Menghong Dai², Xu Wang^{2*}, Yuanhu Pan¹ and Zonghui Yuan^{1,2,5*}

¹ National Reference Laboratory of Veterinary Drug Residues (HZAU) and MAO Key Laboratory for Detection of Veterinary Drug Residues, Huazhong Agricultural University, Wuhan, China, ² MOA Laboratory for Risk Assessment of Quality and Safety of Livestock and Poultry Products, Huazhong Agricultural University, Wuhan, China, ³ College of Life Science, Yangtze University, Jingzhou, China, ⁴ Department of Chemistry, Faculty of Science, University of Hradec Kralove, Hradec Kralove, Czechia, ⁵ Hubei Collaborative Innovation Center for Animal Nutrition and Feed Safety, Wuhan, China

OPEN ACCESS

Edited by:

Wolff Mayer Kirsch,
Loma Linda University Medical
Center, United States

Reviewed by:

David Stec,
University of Mississippi Medical
Center, United States
Salvador Soriano,
Loma Linda University, United States

*Correspondence:

Xu Wang
wangxu@mail.hzau.edu.cn
Zonghui Yuan
yuan5802@mail.hzau.edu.cn

Specialty section:

This article was submitted to
Experimental Pharmacology
and Drug Discovery,
a section of the journal
Frontiers in Pharmacology

Received: 20 December 2017

Accepted: 12 April 2018

Published: 01 May 2018

Citation:

Liu Q, Lei Z, Guo J, Liu A, Lu Q,
Fatima Z, Khaliq H, Shabbir MAB,
Maan MK, Wu Q, Dai M, Wang X,
Pan Y and Yuan Z (2018)
Mequindox-Induced Kidney Toxicity Is
Associated With Oxidative Stress
and Apoptosis in the Mouse.
Front. Pharmacol. 9:436.
doi: 10.3389/fphar.2018.00436

Mequindox (MEQ), belonging to quinoxaline-di-*N*-oxides (QdNOs), is a synthetic antimicrobial agent widely used in China. Previous studies found that the kidney was one of the main toxic target organs of the QdNOs. However, the mechanisms underlying the kidney toxicity caused by QdNOs *in vivo* still remains unclear. The present study aimed to explore the molecular mechanism of kidney toxicity in mice after chronic exposure to MEQ. MEQ led to the oxidative stress, apoptosis, and mitochondrial damage in the kidney of mice. Meanwhile, MEQ upregulated Bax/Bcl-2 ratio, disrupted mitochondrial permeability transition pores, caused cytochrome c release, and a cascade activation of caspase, eventually induced apoptosis. The oxidative stress mediated by MEQ might led to mitochondria damage and apoptosis in a mitochondrial-dependent apoptotic pathway. Furthermore, upregulation of the Nrf2-Keap1 signaling pathway was also observed. Our findings revealed that the oxidative stress, mitochondrial dysfunction, and the Nrf2-Keap1 signaling pathway were associated with the kidney apoptosis induced by MEQ *in vivo*.

Keywords: mequindox, oxidative stress, Nrf2-Keap1, apoptosis, quinoxaline-di-*N*-oxides

INTRODUCTION

Quinoxaline-di-*N*-oxides (QdNOs), consisting of one or two acyclic chain moiety combined with quinoxaline ring, are best known as potential antibacterial agents (Wu et al., 2007; Vicente et al., 2009; Wang et al., 2011a, 2015a, 2016c; Cheng et al., 2015; Liu et al., 2016, 2017). Carbadox (CBX), olaquindox (OLA), quinocetone (QCT), and cyadox (CYA) were the classical members of QdNOs (Wang et al., 2015a,b; Zhang et al., 2015). Due to the potential genotoxic and carcinogenic effect, CBX and OLA had been banned in food-producing animals by European Commission since 1998 (Wang et al., 2016c). Mequindox (MEQ; 3-methyl-2-acetyl-*N*-1,4-dioxyquinoxaline,

Abbreviations: 8-OHdG, 8-hydroxy deoxyguanosine; BUN, blood urea nitrogen; CBX, carbadox; crea, creatinine; CYA, cyadox; GCLC, glutamate-cysteine ligase catalytic subunit; GSH, glutathione; GSH-Px, glutathione peroxidase; GST, glutathione S-transferase; HO-1, hydroxyl radicals; IκB, nuclear factor κB protein; LDH, lactate dehydrogenase; M4, 3-methyl-2-(1-hydroxyethyl) quinoxaline-*N*4-monoxide; M8, 3-methyl-2-(1-hydroxyethyl) quinoxaline-*N*1-monoxide; MDA, malondialdehyde; MEQ, mequindox; *N*1-MEQ, *N*1-desoxymequindox; NQO1, NAD(P)H:quinoneoxidoreductase; OLA, olaquindox; QCT, quinocetone; QdNOs, quinoxaline-di-*N*-oxides; ROS, reactive oxygen species; SOD, superoxide dismutase; TEM, transmission electron microscope; T-SOD, total superoxide dismutase; UA, uric acid.

$C_{11}H_{10}N_2O_3$) (**Figure 1**), a relatively new QdNOs, can effectively improve growth and feed efficiency in animals for its better than other antimicrobial agents in treatment of swine dysentery (*Treponema hyodysenteriae*) (Liu et al., 2010; Ihsan et al., 2011, 2013a; Ding et al., 2012). As a synthetic antimicrobial agent, MEQ had significant antibacterial activities against both Gram-positive and Gram-negative species (Huang et al., 2015).

Previous studies demonstrated that some of the QdNOs such as OLA and CBX exhibited toxicity in the liver, kidney, and adrenal glands (Huang et al., 2010a,b; Ihsan et al., 2010, 2013a,b; Wang et al., 2016b; Liu et al., 2017). Early findings identified the adrenal glands as one of the main targets of QdNOs *in vitro* and *in vivo* (Huang et al., 2009, 2010a,b; Ihsan et al., 2010). MEQ was reported to reduce the output of adrenal aldosterone in pig adrenocortical cells (Huang et al., 2010b), and decreased serum aldosterone in rats (Huang et al., 2010a). The kidney has an important function in some unique physiology and metabolic pathways like the uptake, metabolism, and elimination of drugs (Lohr et al., 1998). Besides adrenal gland, kidney also plays an essential role in fluid-ion balance. However, the previous organ toxicity studies of MEQ only focus on the adrenal gland, while the kidney toxicity is commonly ignored. To date, only one study demonstrated the kidney damage on the male Wistar rats after exposure to MEQ (110 and 275 mg/kg) for up to 180 days, indicating that the kidney was another important target of MEQ (Huang et al., 2010a). However, the mechanism underlying kidney toxicity mediated by MEQ *in vivo*, especially regarding some linked signaling pathways was still not adequately understood.

A lot of evidence suggested that the oxidative stress was closely related to the damages caused by QdNOs, including apoptosis, DNA, and lipid damage (Chowdhury et al., 2004; Azqueta et al., 2007; Liu et al., 2012, 2017; Yang et al., 2013; Zhang et al., 2014; Wang et al., 2015a). The oxidative stress was also considered as the main factor in adrenal gland

(Huang et al., 2009), liver (Wang et al., 2011b; Liu et al., 2017), spleen (Wang et al., 2011b), and testis toxicity (Ihsan et al., 2011) that caused by MEQ *in vivo*. The previous study concluded that MEQ-induced oxidative damage with the changes of reduced glutathione (GSH), superoxide dismutase (SOD), and malondialdehyde (MDA) in kidney (Huang et al., 2010a). Moreover, the oxidative stress was regarded as a molecular mechanism for MEQ to induce adrenal toxicity in H295R cells that originated from a human adrenocortical carcinoma (Wang et al., 2016b). Therefore, it was suspected that the oxidative stress may be involved in the toxicity in mice after chronic exposure to MEQ.

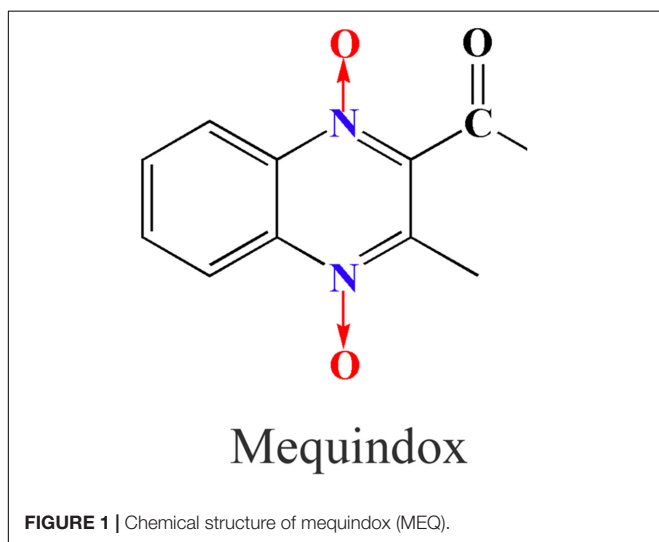
The QdNO-mediated oxidative stress is associated with a large number of biological responses and related cell signaling pathways. It was reported that the apoptosis invoked by OLA was always accompanied by the generation of ROS in renal tubular epithelial cells (HK-2 cells) (Li et al., 2015) and HepG2 cells that are from the liver (Zhang et al., 2011; Zhao et al., 2013, 2015). The apoptosis was observed in HepG2 cells after incubation with QCT (Zhang et al., 2013, 2015). However, whether the oxidative stress that triggered by MEQ-induced apoptosis in the kidney *in vivo* is unknown. Due to the wide use of MEQ in food animal production, it is of great significance to investigate the kidney toxicity mediated by MEQ *in vivo*.

In the present study, we investigated comprehensively the following parameters: the effects of MEQ exposure on body and kidney weight, morphological and ultrastructural changes in kidney; activity of the uric acid (UA), urea, creatinine (crea), blood urea nitrogen (BUN), GSH, total superoxide dismutase (T-SOD), MDA, 8-OHdG, and lactate dehydrogenase (LDH) in the serum; the mRNA expression of some genes in the kidney linked with apoptosis (e.g., caspase 3, caspase 8, caspase 9, and cychrome c), and correlated with oxidative stress (e.g., Nrf-2, GCLC, NQO1, HO-1, GSH-Px, and GST); the protein expression of cleaved caspase 3 and Nrf-2 in the kidney by immunohistochemistry, Western blot, and immunofluorescence assays. The study aimed at providing insight into molecular mechanism of MEQ-induced kidney toxicity *in vivo*, which will help to evaluate MEQ in its clinical use and improve the prudent use of QdNOs for public health.

MATERIALS AND METHODS

Chemical Reagents

Mequindox (MEQ; $C_{11}H_{10}N_2O_3$, CAS No: 60875-16-3, purity 98%) was obtained from Beijing Zhongnongfa Pharmaceutical Co., Ltd. (Huanggang, China). SOD, GSH, 8-OHdG, MDA, and LDH kits were purchased from Nanjing Jiancheng Bioengineering Institute (Nanjing, China). Nrf-2 (D1Z9C) XP Rabbit mAb (12721T) and cleaved caspase 3 (Asp175) antibody (9661T) were purchased from Cell Signaling Technology (United States), and a reagent Western Blot Stripping Buffer (T7135A) was purchased from Takara (Japan). All other chemicals and reagents were of analytical



grade and obtained from Sigma-Aldrich (St. Louis, MO, United States).

Animals and Treatment

Recent studies revealed that the toxicity to liver (Liu et al., 2017) and testis (Liu et al., 2017a,b) were caused by MEQ in Kunming mice, while the kidney toxicity of MEQ in Kunming mice remains poor understood. Thus, the Kunming mice were chosen in this study. A total of 40 specific pathogen-free (SPF) Kunming mice (6–7 weeks old, weighing 30 ± 5 g) were obtained from Center of Laboratory Animals of Hubei Province (Wuhan, China). The individual body weights of the mice were within $\pm 20\%$ of the average. The mice were maintained in a room conditioned at $22 \pm 3^\circ\text{C}$, a relative humidity of $50 \pm 20\%$, and a 12-h light/dark cycle. The current study was approved by the Ethical Committee of the Faculty of Veterinary Medicine (Huazhong Agricultural University). Before treatment, the mice received basic feed and a standard diet from Nuvital Nutrients (Colombo/PR, Brazil), allowed to access to distilled water *ad libitum* for 7 days to evaluate for any signs of disease and weight gain.

According to the Organization for Economic Cooperation and Development (OECD) Guideline 453 and Procedures for toxicological assessment of food in China, the high-dose level should cause some toxic effect performance or damage, and the low-dose group may not show any toxic effects, but should be 1–3 times greater than the clinical dose (GB15193.17, 2003; OECD, 2009). In a previous sub-chronic and chronic toxicity study, MEQ in 110 mg/kg diet made an increase in plasma potassium (K^+) level without growth inhibition, and this dose was determined to be no-observed-adverse-effect level (Ihsan, 2011). Therefore, the 110 mg/kg diet was selected as the high dose, and 55 mg/kg for the middle and 25 mg/kg for the low dose, respectively.

For the experiments, the mice were randomly divided into four groups ($n = 10$), including a control group treated with the basic diet without feed additives and three experimental groups treated with the same diet supplemented with 25, 55, and 110 mg/kg MEQ, respectively. The mice were housed five per group per sex in shoebox cages with hardwood shavings as bedding. Food and water were supplied *ad libitum* and the treatment period lasted for 11 months. During the experimental period, symptoms and mortality were observed and carefully recorded each day. In this study, the use of animals was in compliance with NIH Publication “The Development of Science Based Guidelines for Laboratory Animal Care” (NRC, 2004).

Coefficients and Preparation of Kidney

Following an overnight fast, the mice were weighted and sacrificed. After weighting the body and kidneys, the coefficient of kidney to body weight was calculated as the ratio of kidney (wet weight, mg) to body weight (BW) (g). The kidneys were excised, rinsed in phosphate-buffered saline (PBS), and the left kidney from all mice ($n = 10$) was quickly frozen at -70°C .

Histopathological Examination

All histopathological tests were performed using standard laboratory procedures. The right kidney from the mice ($n = 5$) was preserved in 10% neutral-buffered formalin. After fixation,

the kidneys were embedded in paraffin blocks, then sliced into $5 \mu\text{m}$ in thickness and placed onto glass slides with hematoxylin–eosin (HE) staining. Slides were observed and the photos were taken using an optical microscope (Olympus BX 41, Japan) for morphological alterations.

Observation of Nephrocyte Ultrastructure by Transmission Electron Microscope

The right kidney from other mice ($n = 5$) was fixed by 2.5% glutaraldehyde in 0.1 mol/dm^3 cacodylate buffer for 4 h, then followed by wash three times with 0.1 mol dm^3 cacodylate buffer (pH 7.2–7.4) and put in 1% osmium tetroxide for 1 h. A graded series of ethanol (75, 85, 95, and 100%) was used to dehydrate the specimens and embedded in Epon 812. Ultra-thin sections (70 nm) were contrasted with lead citrate for 10 min and uranyl acetate for 30 min, and then observed with an H-7650 TEM (Hitachi, Japan). The nephrocyte apoptosis was judged according to the nuclear morphology changes (e.g., chromatin fragmentation and condensation).

TUNEL Assay

The right kidney from the mice ($n = 5$) was performed on $4\text{-}\mu\text{m}$ paraffin sections using antigen retrieval for 10 min of boiling in 10 mM citrate buffer (pH 6.0). They were fixed in 4% paraformaldehyde (pH 7.4) at -20°C for 3 min. After washing with PBS, the sections were permeabilized with 0.1% Triton X-100. Then, the samples were washed in PBS and incubated with a terminal deoxynucleotide transferase-mediated dUTP nick end labeling (TUNEL) reagent containing terminal deoxynucleotidyl transferase and fluorescent isothiocyanate dUTP. After incubation, they were stained with $1 \mu\text{g/ml}$ DAPI for 30 min to investigate the cell nucleus by UV light microscopic observations (blue). The kidney samples were analyzed in a drop of PBS under a fluorescence and UV light microscope. All morphometric measurements were observed by at least three independent individuals in a blinded manner.

Biochemical Analysis

For biochemical analysis, the serum aliquots were obtained by placed the blood samples in serum tubes at temperature of 24°C for approximately 30 min. After clotting, the blood tubes were centrifuged at 3000 rpm for 10 min using a Himac CR 21 G centrifuge (Hitachi, Tokyo, Japan). Supernatants were separated out and then stored at -20°C for further analysis. Kidney functions were determined by serum activities of UA, urea, crea, and BUN. All biochemical assays were performed using a Synchron CX4 Clinical System (Beckman Coulter, Brea, CA, United States) according to the manufacturer’s protocol (Beijing Leadman Biochemistry Technology Co., Ltd., Beijing, China).

Oxidative Stress Assay

The effects of MEQ on the activity of 8-OHdG, MDA, GSH, T-SOD, and LDH in the serum were examined. Assays of 8-OHdG, MDA, T-SOD, and GSH levels were performed using commercial kits. The release of LDH was assessed using Synchron

Clinical System CX4 (Beckman Coulter, Brea, CA, United States) according to the manufacturer's directions (Beijing Leadman Biochemistry Technology Co., Ltd., Beijing, China). The data were analyzed according to the manufacturer's instructions.

RNA Extraction and qPCR

Total RNA from the left kidney from all mice ($n = 10$) was extracted using the Trizol Reagent according to the manufacturer's instructions. RNA (1 μ g) was reverse transcribed to cDNA with the use of ReverTra AceTM First Strand cDNA Synthesis Kit (Promega, United States). Synthesized cDNA was used for quantitative real-time polymerase chain reaction (Bio-Rad, United States) by SYBR[®] Premix Ex TaqTM RT-PCR kit (Takara, CodeDRR041 A, Japan). The mRNA expression of the apoptotic cytokines (e.g., caspase 3, caspase 8, caspase 9, cytochrome c, Bcl-2, and Bax), and oxidative stress-related genes (e.g., Nrf-2, HO-1, GCLC, NQO-1, GST-Px, and GST) were determined by real-time quantitative reverse transcriptase-polymerase chain reaction (RT-PCR). Mice specific primers were designed using Primer Express Software according to the software guidelines (Table 1). The primers were manufactured by Nanjing Genescript Co., Ltd. (Nanjing, China). For the 25 μ L PCR reaction, 12.5 μ L SYBR[®] Premix Ex TaqTM, 1.0 μ L of each primer (10 μ M), 2.0 μ L of cDNA, and 8.5 μ L Rnase Freed H₂O were mixed together.

For GSH-Px, HO-1, GCLC, and Caspase 8, the cycling conditions were as follows: step 1, 30 s at 95°C; step 2, 45 cycles at 95°C for 5 s, 55°C for 30 s; step 3, dissociation stage. For Nrf-2, NQO1, GST, caspase 3, Bcl-2, Bax, and cytochrome c, the cycling conditions were as follows: step 1, 30 s at 95°C; step 2, 45 cycles at 95°C for 5 s, 60°C for 30 s; step 3, dissociation stage. For caspase 9, the cycling conditions were as follows: step 1, 30 s at 95°C; step 2, 45 cycles at 95°C for 5 s, 62°C for 30 s; step 3, dissociation stage. In this study, the housekeeping gene β -actin was used as internal calibrator reference gene for expression profiling of apoptotic and oxidative stress-related genes.

Following amplification, the authenticity of the amplified product by its specific melting temperature (T_m) was verified by a melting curve analysis with the complementary computer software. The threshold cycle of gene of interest and housekeeping gene (HK), and the difference between their Ct values (ΔC_t) were counted. Relative quantitative analyses of gene expression were calculated using $2^{-\Delta\Delta C_t}$ data analysis method in accordance with the previous literatures (Huang et al., 2009; Wang et al., 2016b; Liu et al., 2017).

Western Blotting

The Nrf-2 (D1Z9C) XP[®] Rabbit mAb (12721T) and cleaved caspase 3 (Asp175) antibody (9661T) were purchased from Cell Signaling Technology. Total protein of the tissues was extracted according to the manufacturer's recommended

TABLE 1 | PCR primers used in the gene expression analysis.

| Gene name | Description | Primer sequence (5'-3') | Primer size (bp) |
|----------------|--------------------|---------------------------|------------------|
| β -actin | m β -actin-F | CTGTCCCTGTATGCCTCTG | 221 |
| | m β -actin-R | TTGATGTCACGCACGATT | |
| Nrf-2 | mNrf-2-F | TCCTATGCGTGAATCCCAAT | 103 |
| | mNrf-2-R | GCGGCTTGAATGTTTGTCTT | |
| NQO1 | mNQO1-F | TTCTGTGGCTTCCAGGTCTT | 104 |
| | mNQO1-R | TCCAGACGTTTCTTCCATCC | |
| GCLC | mGCLC-F | ATGTGGACACCCGATGCAGTATT | 200 |
| | mGCLC-R | GTCTTGCTTGATGTCAGGATGGTTT | |
| HO-1 | mHO-1-F | GACAGAAGAGGCTAAGACCGC | 213 |
| | mHO-1-R | TGGAGGAGCGGTGTCTGG | |
| GST | mGST-F | CCGCTCTTTGGGGCTTTAT | 191 |
| | mGST-R | GGTTCGTTGGACAGCAGGGT | |
| GSH-Px | mGSH-Px-F | GAAGTGCGAAGTGAATGG | 224 |
| | mGSH-Px-R | TGTCGATGGTACGAAAGC | |
| Caspase-8 | mCaspase-8-F | ATCTGCTGTATCCTATCCCACG | 180 |
| | mCaspase-8-R | AGGCACTCCTTTCTGGAAGTTAC | |
| Caspase-9 | mCaspase-9-F | GCGGTGGTGAGCAGAAAGA | 190 |
| | mCaspase-9-R | CCTGGGAAGGTGGAGTAGGA | |
| Caspase-3 | mCaspase-3-F | CTGACTGGAAGCCGAAACTC | 203 |
| | mCaspase-3-R | GACTGGATGAACCACGACCC | |
| Cytochrome c | mCytochrome c-F | CATCCCTTGACATCGTGCTT | 250 |
| | mCytochrome c-R | GGGTAGTCTGAGTAGCGTCTGG | |
| Bcl-2 | mBcl-2-F | TGTGGTCCATCTGACCCTCC | 224 |
| | mBcl-2-R | ACATCTCCCTGTTGACGCTCT | |
| Bax | mBax-F | GGATGCGTCCACCAAGAAG | 194 |
| | mBax-R | CAAAGTAGAAGAGGGCAACCAC | |

protocol (Vazyme, Nanjing, China). Phenylmethylsulfonyl fluoride (PMSF) was added into radio immunoprecipitation assay (RIPA) lysis buffer, and the final concentration of PMSF was 1 mM. Total protein from the kidney was isolated in a preparation of RIPA lysis buffer, and then a sonic oscillator was used to break the cells or organelles. Next, it was centrifuged at 12000 g for 30 min at 4°C. The protein concentrations were determined using the BCA Protein Assay Kit (Shanghai Beyotime Biotechnology Co., Ltd., Shanghai, China). Samples with equal amounts of protein (50 µg) were loaded for 1-dimensional SDS-PAGE using 12% separating gel and 5% stacking gel. The separated proteins were electrophoretically transferred to a polyvinylidene fluoride (PVDF) (Minipore) membranes in Trans-Blot Cells (Liuyi, Beijing, China). The membranes were blocked with 5% nonfat milk in Tris-buffered saline containing 0.1% Tween-20 (TBS-T) for 1 h and were then immunoblotted with the primary antibody (anti-cleaved caspase 3 antibody at a dilution of 1:1000; anti-Nrf-2 antibody at a dilution of 1:1000) overnight at 4°C. The membranes were washed for 10 min 3 times with TBS-T and then were incubated with horseradish peroxidase-conjugated secondary anti-IgG antibody (diluted 1:5000) (Beyotime Inst. Biotech, Peking, China) at room temperature for 1 h. The membranes were washed for 10 min three times with TBS-T. Immunoreactive bands were visualized with a chemiluminescent substrate (ECL-Plus, Minipore) for 2–5 min. Images were captured with a LAS-4000 luminescent image analyzer (Fujifilm, Tokyo, Japan).

Immunohistochemical Assay

The kidney was dissected out and fixed in 10% neutral-buffered paraformaldehyde, and paraffin blocks were embedded on appropriate glass slides for processing. These were placed into the oven at 58°C, for 10 min, followed by deparaffinization in xylol, rehydration in alcohol at decreasing concentrations, and washing in distilled water and PBS (0.1 M sodium phosphate buffer, pH 7.2) for 5 min. The endogenous peroxidase was blocked with a 3% hydrogen peroxide solution for 30 min, and then washed in distilled water and PBS for 15 min (3 times, 5 min each). The slides were placed in citrate buffer and subjected to steam heat recovery, maintained at 95–100°C for 30 min, and they were then naturally cooled. The glass slides were then washed with PBS (3 times, 5 min each) and incubated with 5% bovine serum albumin (BSA) for 1 h, in a moist chamber at 37°C. After that, the BSA was discarded, and the glass slides were incubated with appropriate primary antibodies (Nrf-2, 1:500; cleaved caspase 3, 1:300), diluted according to the manufacturer's instructions (Santa Cruz or Millipore, United States), overnight at 4°C, in a moist chamber. Negative controls were processed without using the primary antibodies. The glass slides were then washed with PBS (3 times, 5 min each) and incubated with the biotinylated secondary antibody for 1 h at 37°C in the moist chamber. After another wash in PBS (5 times, 5 min each), they were incubated in 0.1% domain antibody (DAB) solution (in 3% hydrogen peroxide). The glass slides were counter stained with hematoxylin for 2 min, and then washed in running water

for 10 min. Finally, the glass slides were washed in distilled water, dehydrated in alcohol (at increasing concentrations), diaphanized in xylol, and mounted on Entelan® for optic microscopy examination.

Immunofluorescence Assay

The kidney samples were performed on 4 µm paraffin sections of kidney using antigen retrieval for 10 min of boiling in 10 mM citrate buffer (pH 6.0). They were fixed in 4% paraformaldehyde (pH 7.4) at –20°C for 3 min. After washing 4 times in PBS, the sections were permeabilized with 0.1% Triton X-100, exposed to the blocking solution (PBS/3% BSA) and incubated with the primary antibodies cleaved caspase 3 and Nrf-2 at 4°C overnight. After four washes in PBS, the sections were incubated with secondary fluorescently labeled antibodies Dylight 594 antibodies for 45 min and then were washed 3 times in PBS. Nuclei were stained using DAPI. Fluorescent images were taken using an AX70 widefield microscope (Olympus). All morphometric measurements were observed by at least three independent individuals in a blinded manner.

Statistical Analysis

All results are expressed as means ± SD. Statistical analysis was examined by SPSS 15.0 software. Group difference was assessed by one-way analysis of variance (ANOVA) followed by least significance difference (LSD) test. The $p < 0.05$ was considered statistically significant.

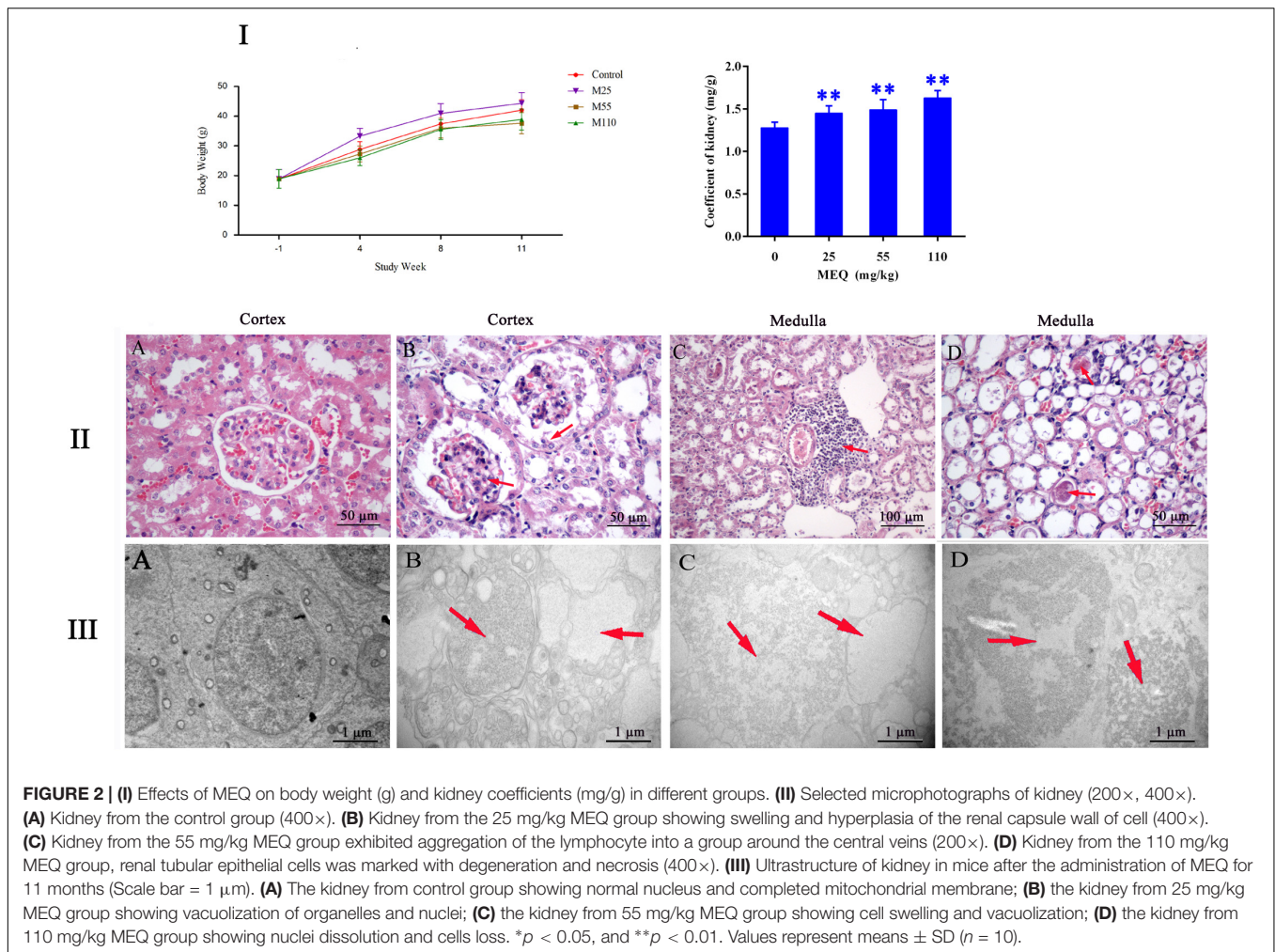
RESULTS

MEQ-Induced Kidney Injury in Mouse Body Weight and Kidney Coefficients

During administration, all the mice were growing and the clinical behaviors, such as food and water consumption in the MEQ-treated groups were as normal as in the control group. The coefficient of kidney to body weight was expressed as milligrams (wet weight of kidneys, mg)/(grams body weight, g). The final body weight and kidney coefficient of mice after administration of MEQ for 11 months were shown in **Figure 2I**. Compared with the controls, significant reductions in body weight were observed in 25, 55, and 110 mg/kg groups ($p < 0.05$ or $p < 0.01$), while the significant increase in kidney coefficients were noted in 25, 55, and 110 mg/kg MEQ groups ($p < 0.01$).

Histopathological Evaluation

The frame of reference as to where in the kidney these slides were obtained in the **Supplementary Figure S1**. As shown in **Figure 2II**, the significant histopathological changes in kidneys were observed in MEQ-treated groups. The glomerular capillaries exhibited expansion, and the renal capsule wall of cell showed swelling and hyperplasia in 25 mg/kg MEQ group (**Figure 2IIB**). Lymphocyte aggregated into a group around the central veins in 55 mg/kg MEQ group (**Figure 2IIC**). In 110 mg/kg MEQ group, renal changes were characterized by degeneration and necrosis of renal tubular epithelial cells with the appearance of protein casts



in the tubular lumen (**Figure 2IID**). This result suggested that the kidney damage was induced by MEQ *in vivo*.

Ultrastructural Changes and Apoptosis Induced by MEQ

The TEM analysis and TUNEL staining were carried out to investigate the ultrastructural changes and apoptosis of kidney induced by MEQ (**Figures 2III, 3**). The kidney in the control group presented normal nuclear morphology and completed mitochondrial membrane (**Figure 2IIIA**). In MEQ-treated groups, cells loss, cell swelling, nuclei dissolution, and mitochondria appeared vacuolization were noted (**Figures 2IIIB,C,D**). Additionally, the obvious apoptosis was also observed in MEQ-treated groups (**Figures 3B,C,D**). These findings revealed the obvious apoptosis and mitochondria damage caused by MEQ in the mouse.

The Changed Serum Biochemical Levels and Oxidative Stress Induced by MEQ

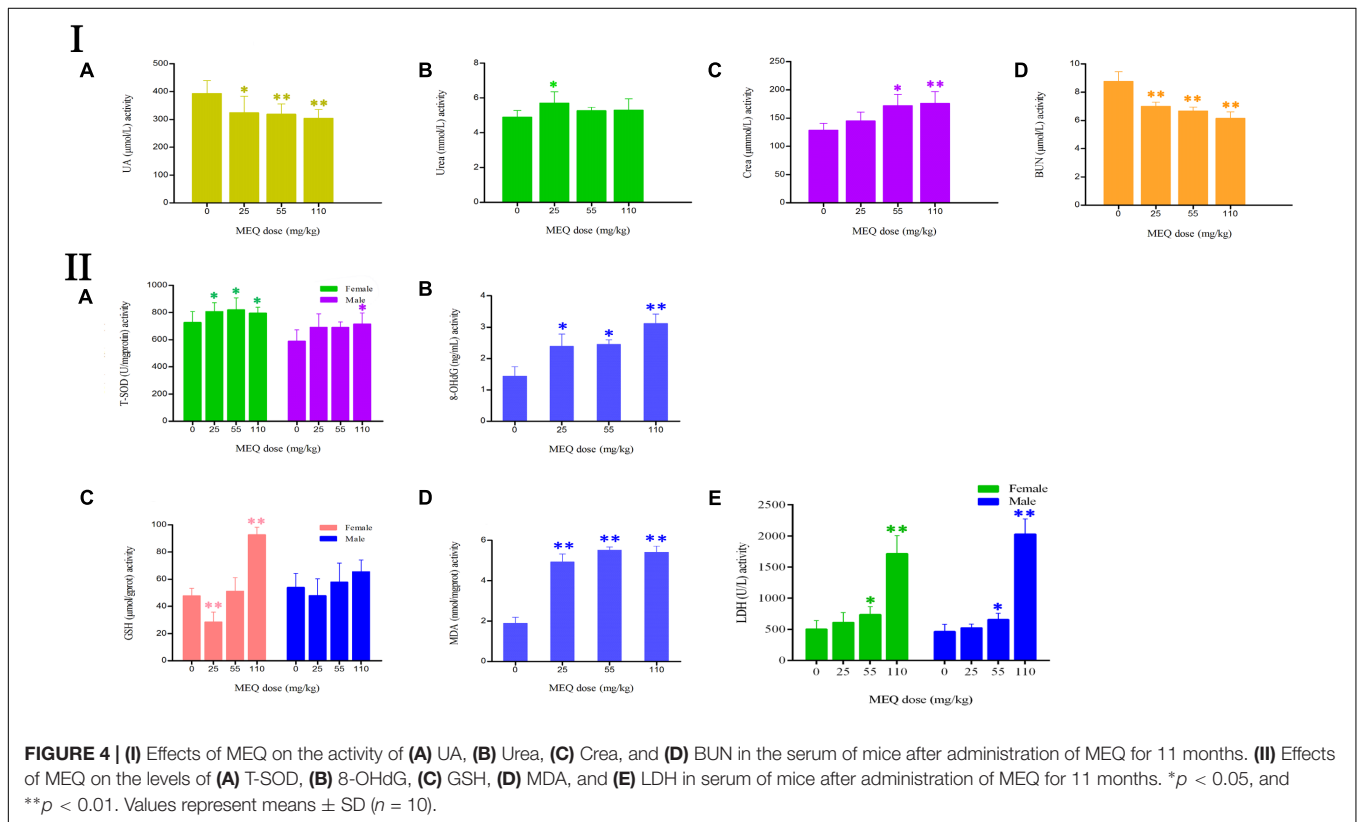
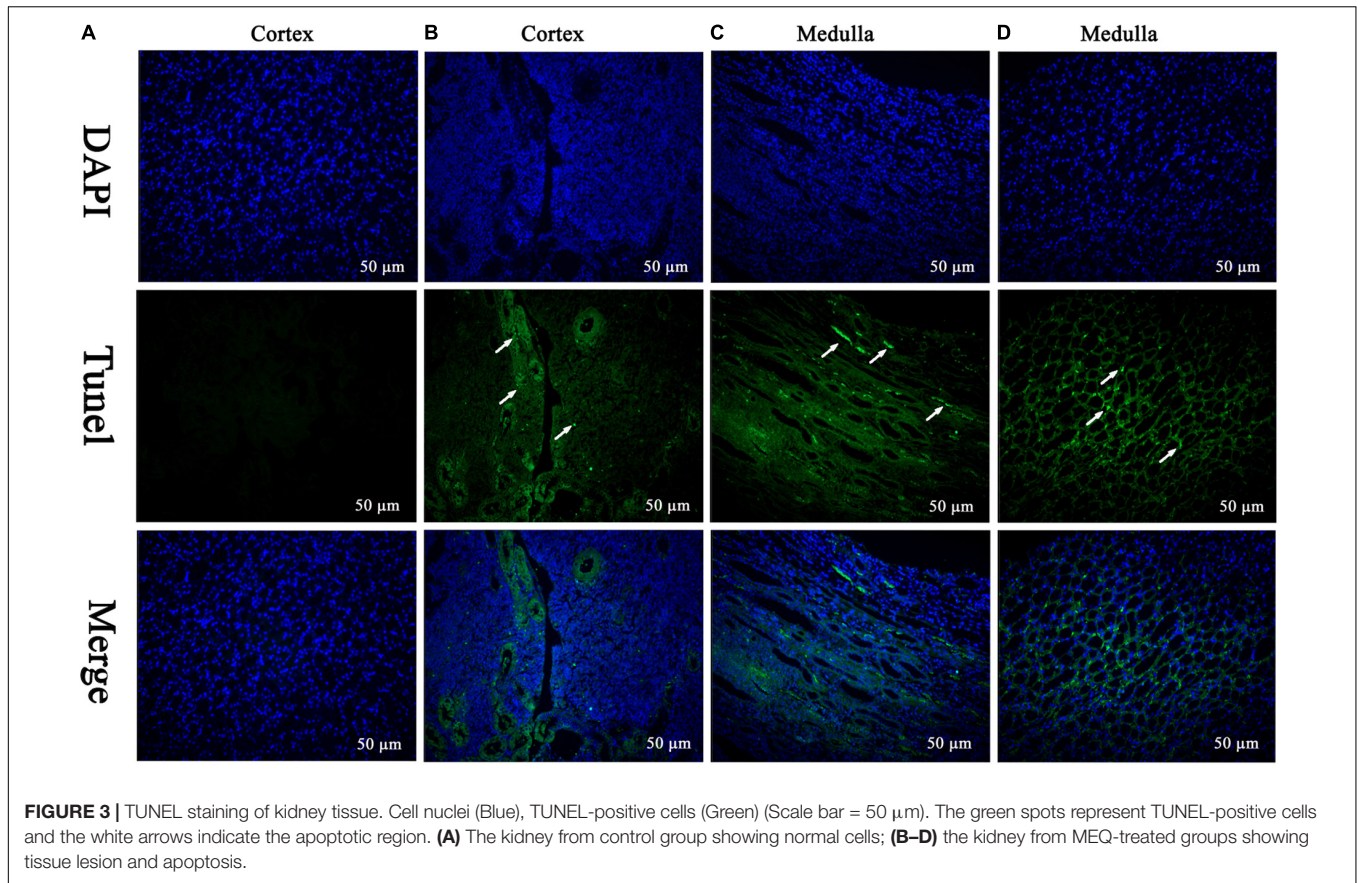
The effect of MEQ on the serum biochemical parameters was presented in **Figure 4I**. In comparison with the control group, the UA and BUN had shown a greatly decreased

in all the MEQ-treated groups ($p < 0.05$ or $p < 0.01$). The significant increased levels of urea and creatinine was found in 25 mg/kg MEQ group ($p < 0.05$), and in 55 and 110 mg/kg MEQ groups ($p < 0.05$ or $p < 0.01$), respectively. The changed serum biochemical parameters demonstrated the chronic kidney disease occurred in mice after exposure to MEQ.

As shown in **Figure 4II**, the levels of 8-OHdG and MDA were markedly increased in the MEQ-treated groups ($p < 0.05$ or $p < 0.01$). The levels of T-SOD were significantly increased on females after exposure to MEQ at 25, 55, and 110 mg/kg groups ($p < 0.05$), and on males at 110 mg/kg ($p < 0.05$), respectively. For the effects of MEQ on the activity of GSH, the significant increased levels were observed in the female at 110 mg/kg group ($p < 0.01$), and significant decreased in the male at 25 mg/kg group ($p < 0.01$). These results show that the oxidative stress was triggered in mice after chronic administration of MEQ.

MEQ-Induced Apoptosis and Activation Nrf2-Keap1 Signaling Pathway

Apoptosis plays an important role in both the physiological process of kidney growth and in different human renal diseases.



To determine the role of apoptosis signal pathway in the mouse kidney after administration of MEQ for 11 months, real-time quantitative RT-PCR was used to demonstrate the changes of the genes including caspase 3, caspase 8, caspase 9, Bcl-2, Bax, and cytochrome c (Figure 5). With increased MEQ doses, there was a significant increase in caspase 3 and caspase 9 ($p < 0.01$). Exposure to MEQ significantly induced the expression of cytochrome c, Bcl-2, and Bax in 55 and 110 mg/kg groups ($p < 0.05$ or $p < 0.01$). A significant increased expression of caspase 8 was observed in 55 and 110 mg/kg MEQ groups ($p < 0.01$), and a marked reduction expression of caspase 8 was observed in 25 mg/kg MEQ group ($p < 0.01$).

The frame of reference as to where in the kidney these slides were obtained in the **Supplementary Figures S2–S7**. Cleaved caspase 3 is a well-characterized cell apoptotic marker, the protein level of cleaved caspase 3 was detected by Western blot (Figure 6I), immunohistochemical analyses (Figure 6II), and immunofluorescence assay (Figure 7), indicating that compared to the control group, treating with MEQ caused increased cleaved caspase 3 expression. Taken together, these results suggested that the apoptosis induced by MEQ in kidney, and the mitochondrial dysfunction and caspase activation was involved in apoptosis mediated by MEQ.

Some oxidative stress-related genes (e.g., Nrf-2, HO-1, NQO1, GCLC, GST-Px, and GST) were determined using real-time quantitative RT-PCR (Figure 5). Exposure to MEQ significantly

induced the expression of Nrf-2 and GSH-Px in the MEQ-treated groups ($p < 0.05$ or $p < 0.01$). An increased expression mRNA level of NQO1 and GST were observed on the doses of 55 and 110 mg/kg MEQ group ($p < 0.01$). There was a significant increased expression of HO-1 and GCLC in 110 mg/kg MEQ group ($p < 0.01$), and an obvious reduction expression of HO-1 and GCLC in 25 and 55 mg/kg MEQ groups ($p < 0.01$).

Accordingly, Western blot (Figure 6I), immunohistochemical analyses (Figure 6II), and immunofluorescence assay (Figure 7) also showed that MEQ-treated groups significantly increased the expression of Nrf-2 compared with those in the control group. These results showed that the activation of Nrf2/Keap1 signaling pathways mediated by MEQ might be a cellular protection response to oxidative stress in kidney.

DISCUSSION

The role of oxidative stress associated with organ toxicity mediated by QdNOs was extensively studied in rats (Huang et al., 2009, 2010a; Ihsan et al., 2010, 2011; Wang et al., 2011b; Yu et al., 2013, 2014) and mice (Wang D. et al., 2011; Zhao et al., 2011; Liu et al., 2017). The kidney has been identified as the main toxic organ target of QdNOs including MEQ. However, unlike other toxicities caused by QdNOs, their effect on kidney is not well studied. The results of present study demonstrated

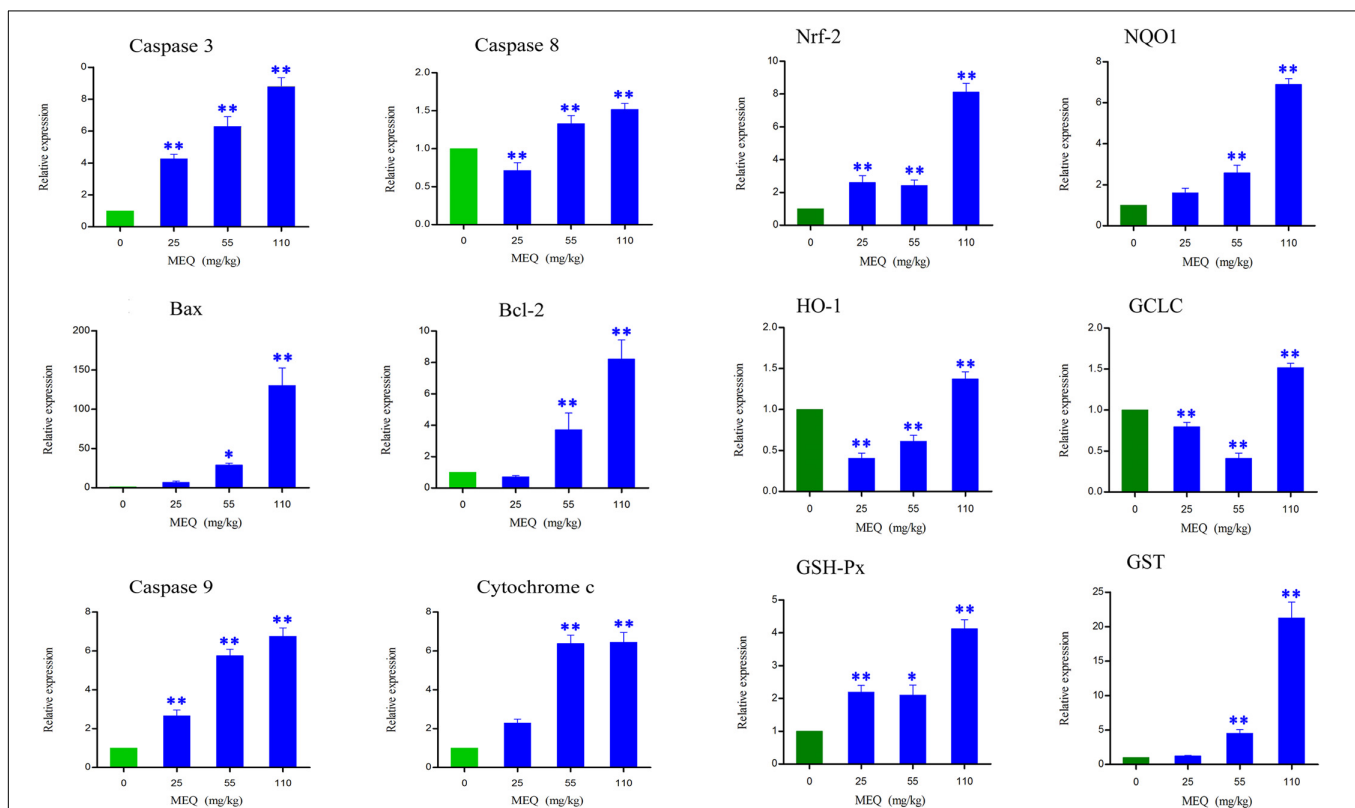


FIGURE 5 | Alterations of Bax, Bcl-2, Caspase 3, Caspase 8, Caspase 9, Cytochrome c, Nrf-2, NQO1, HO-1, GCLC, GSH-Px, and GST mRNA expression by RT-PCR in mouse kidney after administration of MEQ for 11 months. * $p < 0.05$, and ** $p < 0.01$. Values represent means \pm SD ($n = 10$).

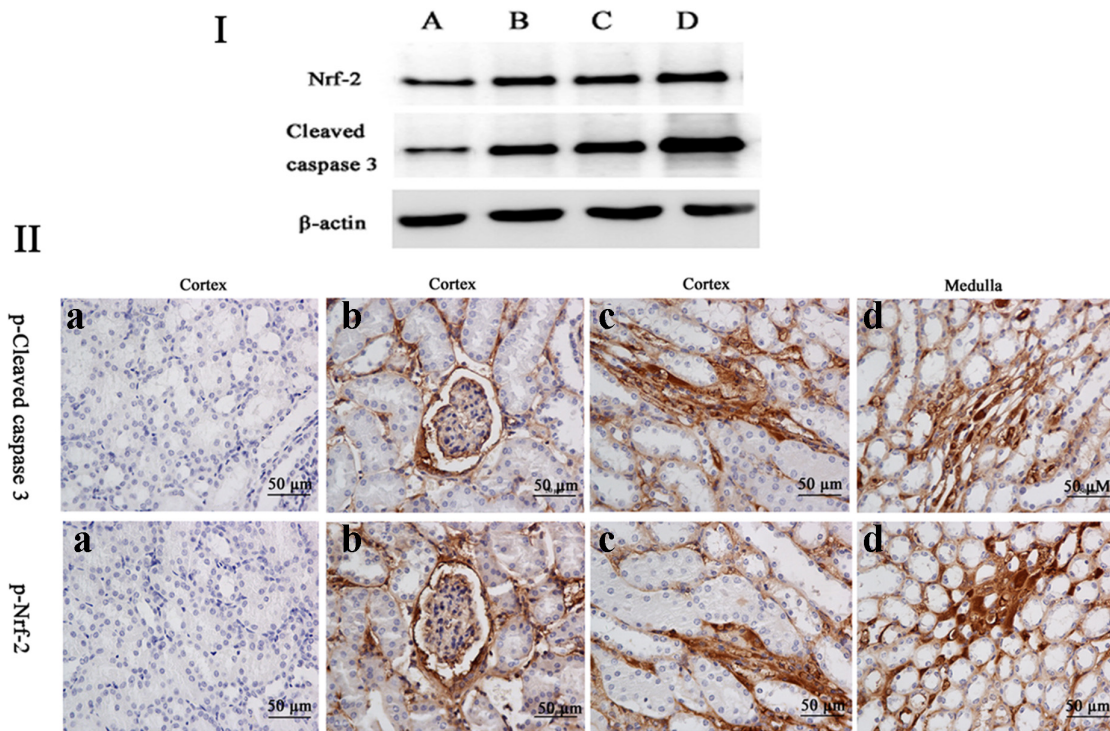


FIGURE 6 | (I) The protein levels of phosphorylated Nrf-2 and cleaved caspases 3 were determined by Western blotting. β -actin was used as an internal control. **(II)** The protein expression of cleaved caspase 3 and Nrf-2 were detected by immunohistochemical assays (the positive reaction of anti-cleaved caspase 3 and anti-Nrf-2 antibody were brown); **(a)** the kidney from the control group, **(b–d)** the kidney from M25, M55, and M110 groups, respectively, showed a positive reaction in the glomerulus and medulla kidney.

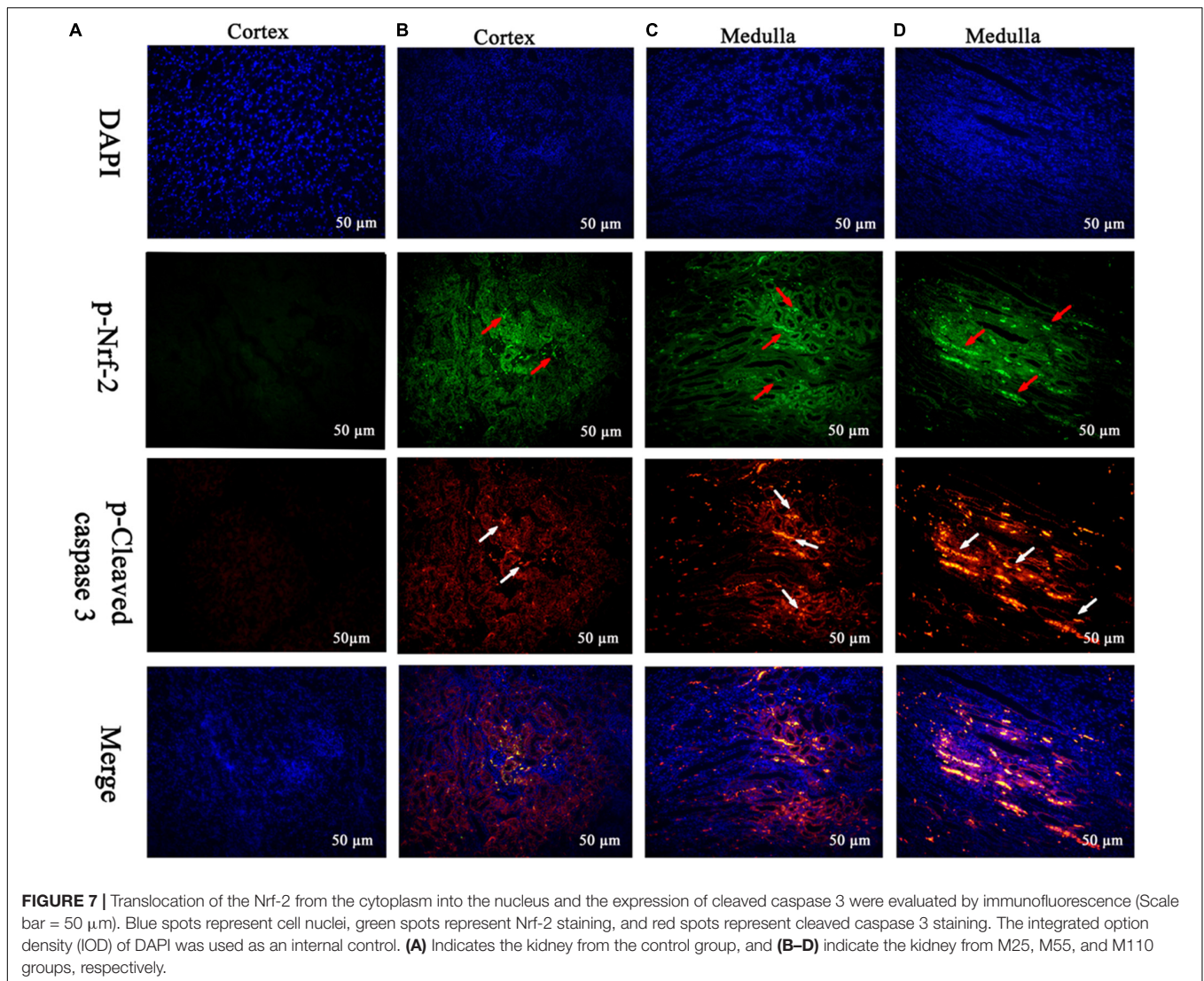
that the oxidative damage was triggered by MEQ, which might be responsible for apoptosis and mitochondrial dysfunction in kidney of mice after the administration of MEQ for 11 months. Additionally, MEQ-induced apoptosis via upregulated Bax/Bcl-2 ratio, caused cytochrome c release and a cascade activation of caspase. Furthermore, the Nrf2-Keap1 signaling pathway might be a protective response to the apoptosis in mice kidney caused by MEQ. This study is of great significance to evaluate MEQ in its clinical use and improve the prudent use of QdNOs for public health.

The kidney was reported to be an important target organ of MEQ, and the main characters of the kidney damage included the cell loss, cell swelling, nuclei shrinkage, hemorrhages, cell atrophy, and vacuolation in the Wistar rats after chronic exposure to MEQ (Huang et al., 2010a). In the present study, a significant reduction in body weight and a significant increase in the kidney coefficients were observed in mice after treatment of MEQ at doses of 25, 55, and 110 mg/kg for 11 months. In serum biochemical analysis, MEQ increased the levels of urea and crea, and reduced the concentration of BUN and UA. The altered levels of these parameters indicated chronic kidney disease in mice. Histopathological evaluation showed obvious kidney damage in MEQ-treated groups, including expansion of glomerular capillaries, swelling, degeneration, and necrosis of renal tubular epithelial cells. In the TUNEL staining and TEM analysis, the obvious apoptosis and ultrastructural changes including

cells loss, cell swelling, nuclei dissolution, and vacuolization of mitochondria were caused by MEQ. The histopathological and TEM observations revealed that MEQ caused damage to cortex and medulla of the kidney. The effect of MEQ was primary on renal tubule and collecting duct. These results demonstrated that apoptosis in kidney occurred after chronic oral administration of MEQ, which confirmed the earlier findings that the kidney was an important toxicity organ target for MEQ *in vivo*.

Previous studies documented that the oxidative stress was closely related to the *in vitro* toxicity caused by QdNOs, such as cytotoxicity, adrenal toxicity, genotoxicity, and apoptosis (Liu et al., 2016, 2017). Long-term MEQ treatment-induced endocrine and reproductive toxicity via oxidative stress with the significant changed levels of SOD, GSH, MDA, and 8-OHdG in male Wistar rats (Ihsan et al., 2011; Liu et al., 2016). A recent study revealed that the oxidative stress played a critical role in the liver toxicity after chronic exposure to MEQ for 11 months (Liu et al., 2017). Herein, our results showed that the levels of MDA, 8-OHdG, T-SOD, GSH, and LDH were significantly increased in the MEQ-treated groups (Figure 5), suggesting an imbalance of redox in mice. This finding revealed that chronic exposure to MEQ invoked oxidative stress in mice, and the oxidative stress was closely related to the organ toxicity mediated by MEQ *in vivo*.

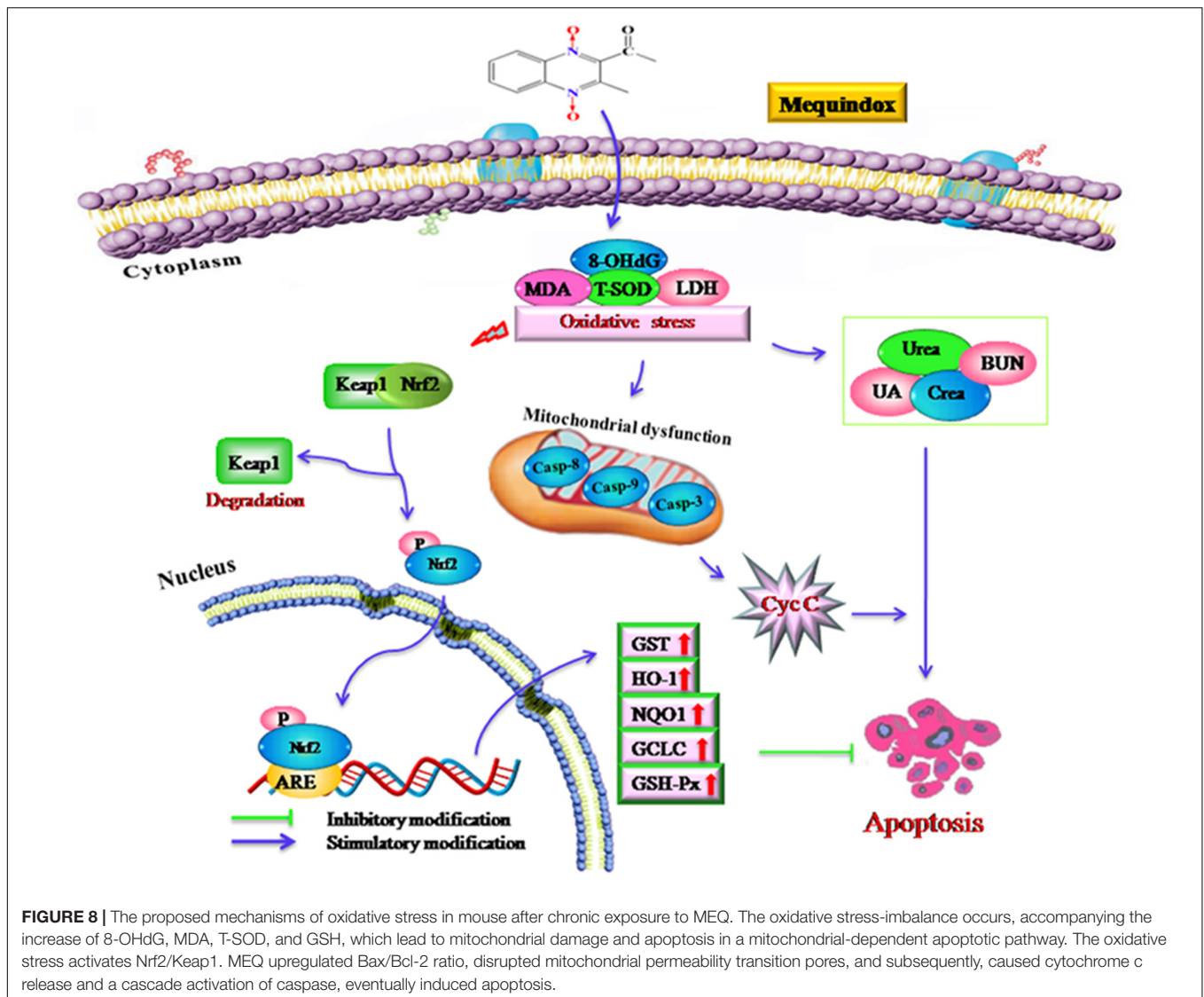
Cleaved caspase 3 is a well-characterized cell apoptotic marker and caspase 9 is a biomarker of mitochondrial apoptosis pathway. The multimeric complex formation of cytochrome c, caspase



8, and caspase 9 activates downstream caspases, leading to apoptosis cell death (Alabsi et al., 2016). Simultaneously, the Bcl-2 family proteins function as central regulators of apoptosis in mammals (Alabsi et al., 2016). In this study, MEQ significantly increased the protein expression of cleaved caspase 3 and mRNA expression of caspase 3, suggesting that the apoptosis was induced by chronic exposure to MEQ in the kidney of mice. Additionally, the mRNA expression of caspase 8 and caspase 9 were significantly increased, indicating a mitochondrial apoptosis pathway invoked by chronic exposure to MEQ. Furthermore, the expression of cytochrome c was increased in MEQ-treated groups, demonstrating that cytochrome c was possibly released into the cytosol, and subsequently, induced the changed of mitochondrial permeability transition pores. In response to a variety of apoptosis stimuli, over-expression of Bcl-2 or Bax blocks cytochrome c release (Li and Wang, 2006). In our study, Bcl-2 and Bax gene expression were overwhelmingly increased and the ratio of Bax/Bcl-2 markedly elevated by MEQ. These results were consistent with the ultrastructural changes of

kidney under TEM observation. Taking together, these findings indicated that the mitochondrial-dependent apoptotic pathway was triggered by MEQ, and MEQ upregulated Bax/Bcl-2 ratio, caused cytochrome c release and a cascade activation of caspase, eventually induced apoptosis.

Apoptosis can be triggered by oxidative stress and the damage to DNA (Skipper et al., 2016). MEQ was reported to induce DNA damage in testis of rats *in vivo*, and increased the level of 8-OHdG in rats (Ihsan et al., 2011) and mice (Liu et al., 2017). In this study, the apoptosis in kidney might be resulted from the oxidative stress and mitochondrial dysfunction mediated by MEQ. Currently, there are two well-characterized caspase-activating cascades: one is initiated by the cell surface death receptor and the other is triggered by changes in mitochondrial integrity (Alabsi et al., 2016). Mitochondria were reported to be a target organelle of QdNOs and extra production of ROS might be result in mitochondrial damage, following with mitochondrial apoptotic pathway (Dai et al., 2015). Herein, the organelle included mitochondrial showed vacuolization in



the MEQ-treated group, demonstrating the destroyed integrity of mitochondria caused by MEQ. Our data revealed that the mitochondrial damage was induced by MEQ, and the oxidative stress and mitochondrial dysfunction might lead to apoptosis in the kidney of mice after administration of MEQ for a long period (Figure 8). Further study should be conducted to investigate the role of mitochondria in the oxidative stress and apoptosis after chronic exposure to MEQ.

The Nrf2-Keap1 pathway was a major cellular defense mechanism against oxidative stress via encoding antioxidant enzymes and phase II detoxifying enzymes (Kobayashi and Yamamoto, 2005; Kimura et al., 2007; Li and Kong, 2009; Pedruzzi et al., 2012). Previous studies suggested that the Nrf-2 was involved in the oxidative damage caused by QCT in rat's liver (Yang et al., 2013; Yu et al., 2013) and NCI-H295R cells (Wang et al., 2016a). Herein, our results demonstrated that the mRNA expression of Nrf-2, GST-Px, NQO1, GST, HO-1, and GCLC were significantly upregulated in the M110

group. Accordingly, the marked increased protein expression of Nrf-2 was noted in MEQ-treated groups. Therefore, the Nrf2-Keap1 signaling pathway was activated by MEQ in mice. Subsequently, the phase II detoxifying enzymes (HO-1, GCLC, and NQO1) and antioxidative enzymes (GST-Px, GST) were generated and these enzymes eventually protected cells from oxidative stress. Interestingly, the mRNA levels of HO-1 and GCLC were significant decreased accompanying the increased of Nrf-2 at the M25 and M55 groups, indicating that the activation of HO-1 and GCLC by Nrf-2 was inhibited, and the further investigation into this phenomenon was needed. Taken together, current study findings revealed that the Nrf2-Keap1 signaling pathway was activated by MEQ, which may be responsible for the protective effect against oxidative damage, apoptosis, and the necrosis in mouse kidney induced by MEQ (Figure 8). Therefore, it was suspected that the Nrf2-Keap1 family was involved in the kidney toxicity caused by MEQ *in vivo*.

Scientists in 2013 reported that the exposure of rats to QCT for 4 weeks with high dose of QCT (2400 mg/kg b.w.) results in significant increased expression of Nrf2 protein in kidney along with the oxidative stress (Yu et al., 2013). However, after rats were treated with QCT for 13 weeks with high dose of QCT (2400 mg/kg b.w.) results in significantly reduced expression of protein Nrf2 and HO-1 along with excessive ROS generation and irreversible oxidative DNA damage, inflammation, and apoptosis in liver, indicated that persistent QCT exposure will inhibit the expression of Nrf2 and HO-1, and aggravate hepatocyte damage (Yu et al., 2014). These findings also suggested a hormesis in the chronic liver disease. Hormesis is a dose-response phenomenon characterized by a low-dose stimulation and a high-dose inhibition (Calabrese et al., 2010). In the present study, a few toxicity-linked parameters, such as serum urea, caspase-8, and GSH, were changed by MEQ not in a dose-dependent manner. It was well documented that the hormetic dose responses were mediated for endogenous cellular defense pathways, including sirtuin and Nrf2 pathways (Calabrese et al., 2010). Therefore, hormesis was suspected to account for these results, and the further study needed to clarify this hypothesis.

CONCLUSION

As shown in **Figure 8**, the current study demonstrated that the kidney was an important toxicity organ target of MEQ *in vivo*, and the oxidative stress and mitochondrial damage were induced in mice after administration of MEQ for 11 months. Additionally, MEQ upregulated Bax/Bcl-2 ratio, caused cytochrome c release, and a cascade activation of caspase, eventually induced apoptosis. Our findings revealed that the oxidative stress might be responsible for mitochondrial damage and apoptosis in a mitochondrial-dependent apoptotic pathway. Furthermore, the present study illustrated that the Nrf2-Keap1 family played a protective role in MEQ-induced redox imbalance damage in the kidney of mice. These findings may contribute to a better understanding of the molecular organ toxicity of MEQ and other QdNOs *in vivo*.

REFERENCES

- Alabsi, A. M., Lim, K. L., Paterson, I. C., Ali-Saeed, R., and Muharram, B. A. (2016). Cell cycle arrest and apoptosis induction via modulation of mitochondrial integrity by Bcl-2 family members and caspase dependence in *Dracaena cinnabari*-treated H400 human oral squamous cell carcinoma. *Biomed. Res. Int.* 2016:4904016. doi: 10.1155/2016/4904016
- Azqueta, A., Arbillaga, L., Pachon, G., Cascante, M., Creppy, E. E., and Lopez de Cerain, A. (2007). A quinoxaline 1,4-di-N-oxide derivative induces DNA oxidative damage not attenuated by vitamin C and E treatment. *Chem Biol. Interact.* 168, 95–105. doi: 10.1016/j.cbi.2007.02.013
- Calabrese, V., Cornelius, C., Dinkova-Kostova, A. T., Calabrese, E. J., and Mattson, M. P. (2010). Cellular stress responses, the hormesis paradigm, and vitagenes: novel targets for therapeutic intervention in neurodegenerative disorders. *Antioxid. Redox Signal.* 13, 1763–1811. doi: 10.1089/ars.2009.3074
- Cheng, G., Li, B., Wang, C., Zhang, H., Liang, G., Weng, Z., et al. (2015). Systematic and molecular basis of the antibacterial action of quinoxaline 1,4-Di-N-oxides

AUTHOR CONTRIBUTIONS

ZY conceived the idea; XW analyzed and discussed the data; QLi analyzed and discussed the data and wrote the paper; ZL performed and revised the experiments; AL performed the experiments; QW and MD revised the paper. All the authors discussed the results and contributed to the final manuscript.

FUNDING

This work was supported by the National Key Research and Development Program of China (2017YFD0501405), Grants from 2015 National Risk Assessment of Quality and Safety of Livestock and Poultry Products (GJFP2015008), and Research on the detection standard of veterinary drug residue (2662015PY021), as well as the long-term development plan UHK.

SUPPLEMENTARY MATERIAL

The Supplementary Material for this article can be found online at: <https://www.frontiersin.org/articles/10.3389/fphar.2018.00436/full#supplementary-material>

FIGURE S1 | Selected microphotographs of kidney in M110 group.

FIGURE S2 | Protein expression of cleaved-caspase 3 detected by immunohistochemical assays in M25 group.

FIGURE S3 | Protein expression of cleaved-caspase 3 detected by immunohistochemical assays in M55 group.

FIGURE S4 | Protein expression of cleaved-caspase 3 detected by immunohistochemical assays in M110 group.

FIGURE S5 | Protein expression of Nrf-2 detected by immunohistochemical assays in M25 group.

FIGURE S6 | Protein expression of Nrf-2 detected by immunohistochemical assays in M55 group.

FIGURE S7 | Protein expression of Nrf-2 detected by immunohistochemical assays in M110 group.

against *Escherichia coli*. *PLoS One* 10:e0136450. doi: 10.1371/journal.pone.0136450

Chowdhury, G., Kotandeniya, D., Daniels, J. S., Barnes, C. L., and Gates, K. S. (2004). Enzyme-activated, hypoxia-selective DNA damage by 3-amino-2-quinoxalinecarbonitrile 1,4-di-N-oxide. *Chem. Res. Toxicol.* 17, 1399–1405. doi: 10.1021/tx049836w

Dai, C. S., Tang, S. S., Deng, S. J., Zhang, S., Zhou, Y., Velkov, T., et al. (2015). Lycopene attenuates colistin-induced nephrotoxicity in mice via activation of the Nrf2/HO-1 pathway. *Antimicrob. Agents Chemother.* 59, 579–585. doi: 10.1128/AAC.03925-14

Ding, H., Liu, Y., Zeng, Z., Si, H., Liu, K., Liu, Y., et al. (2012). Pharmacokinetics of mequindox and one of its major metabolites in chickens after intravenous, intramuscular and oral administration. *Res. Vet. Sci.* 93, 374–377. doi: 10.1016/j.rvsc.2011.07.007

GB15193.17 (2003). *Chronic Toxicity and Carcinogenicity Study*. Haidian District: National Institute of Standards of the People's Republic of China, 109–113.

- Huang, L., Yin, F., Pan, Y., Chen, D., Li, J., Wan, D., et al. (2015). Metabolism, distribution, and elimination of mequindox in pigs, chickens, and rats. *J. Agric. Food Chem.* 63, 9839–9849. doi: 10.1021/acs.jafc.5b02780
- Huang, X. J., Ihsan, A., Wang, X., Dai, M. H., Wang, Y. L., Su, S. J., et al. (2009). Long-term dose-dependent response of Mequindox on aldosterone, corticosterone and five steroidogenic enzyme mRNAs in the adrenal of male rats. *Toxicol. Lett.* 191, 167–173. doi: 10.1016/j.toxlet.2009.08.021
- Huang, X. J., Wang, X., Ihsan, A., Liu, Q., Xue, X. J., Su, S. J., et al. (2010a). Interactions of NADPH oxidase, renin-angiotensin-aldosterone system and reactive oxygen species in mequindox-mediated aldosterone secretion in Wistar rats. *Toxicol. Lett.* 198, 112–118. doi: 10.1016/j.toxlet.2010.05.013
- Huang, X. J., Zhang, H. H., Wang, X., Huang, L. L., Zhang, L. Y., Yan, C. X., et al. (2010b). ROS mediated cytotoxicity of porcine adrenocortical cells induced by QdNOs derivatives in vitro. *Chem. Biol. Interact.* 185, 227–234. doi: 10.1016/j.cbi.2010.02.030
- Ihsan, A. (2011). *Preclinical Toxicology of Mequindox*. Ph.D. thesis, Huazhong Agricultural University, Wuhan.
- Ihsan, A., Wang, X., Huang, X. J., Liu, Y., Liu, Q., Zhou, W., et al. (2010). Acute and subchronic toxicological evaluation of Mequindox in Wistar rats. *Regul. Toxicol. Phar.* 57, 307–314. doi: 10.1016/j.yrtph.2010.03.011
- Ihsan, A., Wang, X., Liu, Z., Wang, Y., Huang, X., Liu, Y., et al. (2011). Long-term mequindox treatment induced endocrine and reproductive toxicity via oxidative stress in male Wistar rats. *Toxicol. Appl. Pharm.* 252, 281–288. doi: 10.1016/j.taap.2011.02.020
- Ihsan, A., Wang, X., Tu, H.-G., Zhang, W., Dai, M.-H., Peng, D.-P., et al. (2013a). Genotoxicity evaluation of Mequindox in different short-term tests. *Food Chem. Toxicol.* 51, 330–336. doi: 10.1016/j.fct.2012.10.003
- Ihsan, A., Wang, X., Zhang, W., Tu, H., Wang, Y., Huang, L., et al. (2013b). Genotoxicity of quinocetone, cyadox and olaquindox in vitro and in vivo. *Food Chem. Toxicol.* 59, 207–214. doi: 10.1016/j.fct.2013.06.008
- Kimura, M., Yamamoto, T., Zhang, J., Itoh, K., Kyo, M., Kamiya, T., et al. (2007). Molecular basis distinguishing the DNA binding profile of Nrf2-Maf heterodimer from that of Maf homodimer. *J. Biol. Chem.* 282, 33681–33690. doi: 10.1074/jbc.M706863200
- Kobayashi, M., and Yamamoto, M. (2005). Molecular mechanisms activating the Nrf2-Keap1 pathway of antioxidant gene regulation. *Antioxid. Redox Signal.* 7, 385–394. doi: 10.1089/ars.2005.7.385
- Li, W., and Kong, A. N. (2009). Molecular mechanisms of Nrf2-mediated antioxidant response. *Mol. Carcinog.* 48, 91–104. doi: 10.1002/mc.20465
- Li, Z., and Wang, J. (2006). A forskolin derivative, FSK88, induces apoptosis in human gastric cancer BGC823 cells through caspase activation involving regulation of Bcl-2 family gene expression, dissipation of mitochondrial membrane potential and cytochrome c release. *Cell Biol. Int.* 30, 940–946. doi: 10.1016/j.cellbi.2006.06.015
- Li, Z., Yu, C., Chen, X., Zhang, B., Cao, P., Li, B., et al. (2015). Research on olaquindox induced endoplasmic reticulum stress related apoptosis on nephrotoxicity. *J. Hygiene Res.* 44, 444–450.
- Liu, J., Ouyang, M., Jiang, J., Mu, P., Wu, J., Yang, Q., et al. (2012). Mequindox induced cellular DNA damage via generation of reactive oxygen species. *Mutat. Res.* 741, 70–75. doi: 10.1016/j.mrgentox.2011.10.012
- Liu, Q., Lei, Z., Dai, M., Wang, X., and Yuan, Z. (2017a). Toxic metabolites, Sertoli cells and Y chromosome related genes are potentially linked to the reproductive toxicity induced by mequindox. *Oncotarget* 8, 87512–87528. doi: 10.18632/oncotarget.20916
- Liu, Q., Lei, Z., Huang, A., Lu, Q., Wang, X., Ahmed, S., et al. (2017b). Mechanisms of the testis toxicity induced by chronic exposure to mequindox. *Front. Pharmacol.* 8:679. doi: 10.3389/fphar.2017.00679
- Liu, Q., Lei, Z., Huang, A., Wu, Q., Xie, S., Awais, I., et al. (2017). Toxic metabolites, MAPK and Nrf2/Keap1 signaling pathways involved in oxidative toxicity in mice liver after chronic exposure to Mequindox. *Sci. Rep.* 7:41854. doi: 10.1038/srep41854
- Liu, Q., Zhang, J., Luo, X., Ihsan, A., Liu, X., Dai, M., et al. (2016). Further investigations into the genotoxicity of quinoxaline-di-N-oxides and their primary metabolites. *Food Chem. Toxicol.* 93, 145–157. doi: 10.1016/j.fct.2016.04.029
- Liu, Z. Y., Huang, L. L., Chen, D. M., and Yuan, Z. H. (2010). Metabolism of mequindox in liver microsomes of rats, chicken and pigs. *Rapid Commun. Mass Spectrom.* 24, 909–918. doi: 10.1002/rcm.4460
- Lohr, J. W., Willsky, G. R., and Acara, M. A. (1998). Renal drug metabolism. *Pharmacol. Rev.* 50, 107–141.
- NRC (2004). *The Development of Science based Guidelines for Laboratory Animal Care, Proceedings of the November 2003 International Workshop*. Washington, DC: National Academy Press.
- OECD (2009). *Guideline for the Testing of Chemicals. Guideline 453: Combined Chronic Toxicity/Carcinogenicity Studies*. OECD: Paris. doi: 10.1787/9789264076457-en
- Pedruzzi, L. M., Stockler-Pinto, M. B., Leite, M. Jr., and Mafra, D. (2012). Nrf2-keap1 system versus NF-kappaB: the good and the evil in chronic kidney disease? *Biochimie* 94, 2461–2466. doi: 10.1016/j.biochi.2012.07.015
- Skipper, A., Sims, J. N., Yedjou, C. G., and Tchounwou, P. B. (2016). Cadmium chloride induces DNA damage and apoptosis of human liver carcinoma cells via oxidative stress. *Int. J. Environ. Res. Public Health* 13, 88–93. doi: 10.3390/ijerph13010088
- Vicente, E., Perez-Silanes, S., Lima, L. M., Ancizu, S., Burguete, A., Solano, B., et al. (2009). Selective activity against *Mycobacterium tuberculosis* of new quinoxaline 1,4-di-N-oxides. *Bioorg. Med. Chem.* 17, 385–389. doi: 10.1016/j.bmc.2008.10.086
- Wang, D., Zhong, Y., Luo, X., Wu, S., Xiao, R., Bao, W., et al. (2011). Pu-erh black tea supplementation decreases quinocetone-induced ROS generation and oxidative DNA damage in Balb/c mice. *Food Chem. Toxicol.* 49, 477–484. doi: 10.1016/j.fct.2010.11.028
- Wang, X., Bai, Y., Cheng, G., Ihsan, A., Zhu, F., Wang, Y., et al. (2016a). Genomic and proteomic analysis of the inhibition of synthesis and secretion of aldosterone hormone induced by quinocetone in NCI-H295R cells. *Toxicology* 350–352, 1–14. doi: 10.1016/j.tox.2016.03.005
- Wang, X., Fang, G. J., Wang, Y. L., Ihsan, A., Huang, L. L., Zhou, W., et al. (2011a). Two generation reproduction and teratogenicity studies of feeding cyadox in Wistar rats. *Food Chem. Toxicol.* 49, 1068–1079. doi: 10.1016/j.fct.2011.01.014
- Wang, X., Huang, X. J., Ihsan, A., Liu, Z. Y., Huang, L. L., Zhang, H. H., et al. (2011b). Metabolites and JAK/STAT pathway were involved in the liver and spleen damage in male Wistar rats fed with mequindox. *Toxicology* 280, 126–134. doi: 10.1016/j.tox.2010.12.001
- Wang, X., Wan, D., Ihsan, A., Liu, Q., Cheng, G., Li, J., et al. (2015a). Mechanism of adrenocortical toxicity induced by quinocetone and its bidesoxy-quinocetone metabolite in porcine adrenocortical cells in vitro. *Food Chem. Toxicol.* 84, 115–124. doi: 10.1016/j.fct.2015.08.016
- Wang, X., Yang, C., Ihsan, A., Luo, X., Guo, P., Cheng, G., et al. (2016b). High risk of adrenal toxicity of N1-desoxy quinoxaline 1,4-dioxide derivatives and the protection of oligomeric proanthocyanidins (OPC) in the inhibition of the expression of aldosterone synthetase in H295R cells. *Toxicology* 341–343, 1–16. doi: 10.1016/j.tox.2016.01.005
- Wang, X., Yang, P. P., Li, J., Ihsan, A., Liu, Q. Y., Cheng, G. Y., et al. (2016c). Genotoxic risk of quinocetone and its possible mechanism in in-vitro studies. *Toxicol. Res.* 5, 446–460. doi: 10.1039/C1035TX00341E
- Wang, X., Zhang, H., Huang, L., Pan, Y., Li, J., Chen, D., et al. (2015b). Deoxidation rates play a critical role in DNA damage mediated by important synthetic drugs, quinoxaline 1,4-dioxides. *Chem. Res. Toxicol.* 28, 470–481. doi: 10.1021/tx5004326
- Wu, Y., Yu, H., Wang, Y., Huang, L., Tao, Y., Chen, D., et al. (2007). Development of a high-performance liquid chromatography method for the simultaneous quantification of quinoxaline-2-carboxylic acid and methyl-3-quinoxaline-2-carboxylic acid in animal tissues. *J. Chromatogr. A* 1146, 1–7. doi: 10.1016/j.chroma.2006.11.024
- Yang, W., Fu, J., Xiao, X., Yan, H., Bao, W., Wang, D., et al. (2013). Quinocetone triggers oxidative stress and induces cytotoxicity and genotoxicity in human

- peripheral lymphocytes of both genders. *J. Sci. Food Agric.* 93, 1317–1325. doi: 10.1002/jsfa.5891
- Yu, M., Wang, D., Xu, M. J., Liu, Y., Wang, X., Liu, J., et al. (2014). Quinocetone-induced Nrf2/HO-1 pathway suppression aggravates hepatocyte damage of Sprague-Dawley rats. *Food Chem. Toxicol.* 69, 210–219. doi: 10.1016/j.fct.2014.04.026
- Yu, M., Xu, M. J., Liu, Y., Yang, W., Rong, Y., Yao, P., et al. (2013). Nrf2/ARE is the potential pathway to protect Sprague-Dawley rats against oxidative stress induced by quinocetone. *Regul. Toxicol. Pharm.* 66, 279–285. doi: 10.1016/j.yrtph.2013.04.005
- Zhang, C. M., Wang, C. C., Tang, S. S., Sun, Y., Zhao, D. X., Zhang, S., et al. (2013). TNFR1/TNF-alpha and mitochondria interrelated signaling pathway mediates quinocetone-induced apoptosis in HepG2 cells. *Food Chem. Toxicol.* 62, 825–838. doi: 10.1016/j.fct.2013.10.022
- Zhang, K., Wang, X., Wang, C., Zheng, H., Li, T., Xiao, S., et al. (2015). Investigation of quinocetone-induced mitochondrial damage and apoptosis in HepG2 cells and compared with its metabolites. *Environ. Toxicol. Pharmacol.* 39, 555–567. doi: 10.1016/j.etap.2015.01.017
- Zhang, K., Zheng, W., Zheng, H., Wang, C., Wang, M., Li, T., et al. (2014). Identification of oxidative stress and responsive genes of HepG2 cells exposed to quinocetone, and compared with its metabolites. *Cell Biol. Toxicol.* 30, 313–329. doi: 10.1007/s10565-014-9287-0
- Zhang, T., Tang, S. S., Jin, X., Liu, F. Y., Zhang, C. M., Zhao, W. X., et al. (2011). c-Myc influences olaquindox-induced apoptosis in human hepatoma G2 cells. *Mol. Cell. Biochem.* 354, 253–261. doi: 10.1007/s11010-011-0825-2
- Zhao, D., Wang, C., Tang, S., Zhang, C., Zhang, S., Zhou, Y., et al. (2015). Reactive oxygen species-dependent JNK downregulated olaquindox-induced autophagy in HepG2 cells. *J. Appl. Toxicol.* 35, 709–716. doi: 10.1002/jat.3022
- Zhao, W. X., Tang, S. S., Jin, X., Zhang, C. M., Zhang, T., Wang, C. C., et al. (2013). Olaquindox-induced apoptosis is suppressed through p38 MAPK and ROS-mediated JNK pathways in HepG2 cells. *Cell Biol. Toxicol.* 29, 229–238. doi: 10.1007/s10565-013-9249-y
- Zhao, X. J., Huang, C., Lei, H., Nie, X., Tang, H., and Wang, Y. (2011). Dynamic metabolic response of mice to acute mequindox exposure. *J. Proteome Res.* 10, 5183–5190. doi: 10.1021/pr2006457

Conflict of Interest Statement: The authors declare that the research was conducted in the absence of any commercial or financial relationships that could be construed as a potential conflict of interest.

The reviewer SS and handling Editor declared their shared affiliation.

Copyright © 2018 Liu, Lei, Guo, Liu, Lu, Fatima, Khaliq, Shabbir, Maan, Wu, Dai, Wang, Pan and Yuan. This is an open-access article distributed under the terms of the Creative Commons Attribution License (CC BY). The use, distribution or reproduction in other forums is permitted, provided the original author(s) and the copyright owner are credited and that the original publication in this journal is cited, in accordance with accepted academic practice. No use, distribution or reproduction is permitted which does not comply with these terms.